J|A|C|S
ARTICLES
Published on Web 12/28/2001

Time-Resolved Spectroscopic Studies of B_{12} Coenzymes: A Comparison of the Primary Photolysis Mechanism in Methyl-, Ethyl-, *n*-Propyl-, and 5′-Deoxyadenosylcobalamin

Allwyn G. Cole, Laurie M. Yoder, Joseph J. Shiang, Neil A. Anderson, Larry A. Walker, II, Mark M. Banaszak Holl, and Roseanne J. Sension*

Contribution from the Department of Chemistry, University of Michigan, Ann Arbor, Michigan 48109-1055

Received July 3, 2001

Abstract: An ultrafast transient absorption study of the primary photolysis of ethyl- and *n*-propylcobalamin in water is presented. Data have been obtained for two distinct excitation wavelengths, 400 nm at the edge of the UV γ-band absorption, and 520 nm in the strong visible $\alpha\beta$-band absorption. These data are compared with results reported earlier for the B_{12} coenzymes, methyl- and adenosylcobalamin. The data obtained for ethylcobalamin and *n*-propylcobalamin following excitation at 400 nm demonstrate the formation of one major photoproduct on a picosecond time scale. This photoproduct is spectroscopically identifiable as a cob(II)alamin species. Excitation of methyl-, ethyl-, and *n*-propylcobalamin at 520 nm in the low-lying $\alpha\beta$ absorption band results in bond homolysis proceeding via a bound cob(III)alamin MLCT state. For all of the cobalamins studied here competition between geminate recombination of caged radical pairs and cage escape occurs on a time scale of 500 to 700 ps. The rate constants for geminate recombination in aqueous solution fall within a factor of 2 between 0.76 and 1.4 ns^{-1}. Intrinsic cage escape occurs on time scales ranging from $\leq$0.5 ns for methyl radical to 2.3 ns for adenosyl, the largest radical studied. The solvent caging correlates well with the size of the radical following anticipated trends: $0 \leq F_C \leq 0.3$ for methyl radical, 0.4 for ethyl radical, 0.57 for *n*-propyl radical, and 0.72 for adenosyl radical.

Introduction

The B_{12}-dependent enzymes may be divided into two broad categories distinguished by the identity of the specific form of the B_{12} coenzyme involved: methyltransferase enzymes utilize a methylcobalamin B_{12} cofactor, while mutase enzymes utilize a 5′-deoxyadenosylcobalamin B_{12} cofactor. The reaction mechanism in the methyltransferase enzymes involves heterolytic cleavage of the carbon−cobalt bond to produce a cob(I)alamin intermediate species.[1,2] In contrast, the mechanism in B_{12}-dependent mutase enzymes involves homolytic cleavage of the carbon−cobalt bond to form cob(II)alamin and an adenosyl radical (Ado•).[2,3] An important, but as yet unanswered, question in B_{12} chemistry is how carbon−cobalt bond reactivity can be directed so differently in the methyl- and adenosylcobalamin coenzymes. In particular, is the cleavage pattern a result of the enzymatic environment or an intrinsic property of the alkylcobalamin?

Alkyl ligands are often assumed to be interchangeable in experimental and theoretical model studies of bond homolysis in cobalamins.[4] Indeed, interchange of methyl, ethyl, *n*-propyl, and adenosyl groups bound to the cobalt in an alkylcobalamin has only a modest effect on the spectroscopic observables. The prevailing similarities are apparent in steady-state electronic and vibrational spectroscopy. In the progression from methyl- to ethylcobalamin the visible $\alpha\beta$-absorption band of the cobalamin undergoes a 10 nm blue shift from 520 to 510 nm, with a concomitant increase in intensity in the 460−400 nm region between the $\alpha\beta$ and γ bands (see Figure 1). Further extension of the alkyl radical from ethyl to *n*-propyl leaves the observed absorption spectrum essentially unchanged. It is difficult to make a direct correlation between these properties and the alkyl radical, as the UV−visible absorption spectrum of adenosylcobalamin bears more resemblance to the methylcobalamin spectrum than to the ethyl- and *n*-propylcobalamin spectra, although the increase in intensity between 460 and 400 nm is preserved.

In an elegant series of measurements reported by Spiro and co-workers, Resonance Raman spectroscopy has been used to investigate the effect of alkyl ligands on the carbon−cobalt bond.[5−8] The frequency of the C−Co stretch is observed to

* Address correspondence to this author. E-mail: rsension@umich.edu.

(1) Banerjee, R. V.; Matthews, R. G. *FASEB J.* **1990**, *4*, 1450−1459.
(2) Ludwig, M. L.; Matthews, R. G. *Annu. Rev. Biochem.* **1997**, *66*, 269−313
(3) Marsh, E. N. G. *BioEssays* **1995**, *17*, 431−441.
(4) For example: Salem, L.; Eisenstein, O.; Anh, N. T.; Burgi, H. B.; Devaquet, A.; Segal, G.; Veillard. A. *Nouv. J. Chim.* **1977**, *1*, 335., Christianson, D. W.; Lipscomb, W. N. *J. Am. Chem. Soc.* **1985**, *107*, 2682. Zhu, L.; Kostic. N. M. *Inorg. Chem.* **1987**, *26*, 4194. Hansen, L. M.; Pavan Kumar, P. N. V.; Marynick D. S. *Inorg. Chem.* **1994**, *33*, 728. Kruppa, A. I.; Taraban, M. B.; Leshina, T. V.; Natarajan, E.; Grissom, C. B. *Inorg. Chem.* **1997**, *36*, 758.
(5) Dong, S.; Padmakumar, R.; Banerjee, R.; Spiro, T. G. *J. Am. Chem. Soc.* **1996**, *118*, 9182−9183.
(6) Dong, S.; Padmakumar, R.; Banerjee, R.; Spiro, T. G. *Inorg. Chim. Acta* **1998**, *270*, 392−398.
(7) Dong, S.; Padmakumar, R.; Maiti, N.; Banerjee, R.; Spiro, T. G. *J. Am. Chem. Soc.* **1998**, *120*, 9947−9948.

10.1021/ja011628s CCC: $22.00

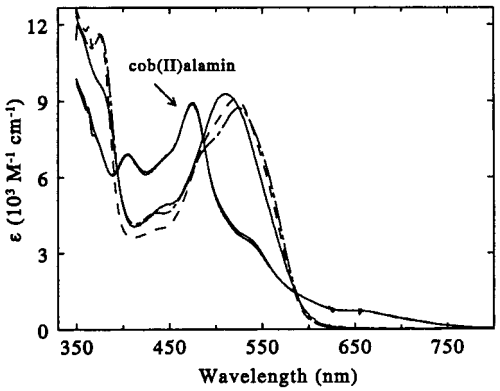

Figure 1. UV−visible absorption spectra of methylcobalamin (dashed line) and *n*-propylcobalamin (solid line) along with the cob(II)alamin spectrum generated by steady state photolysis of each (two nearly identical solid lines labeled in the figure). Note that while there is considerable uncertainty in the absolute molar extinction coefficients for the these spectra, the relative intensities are much more precise. The UV−visible absorption spectrum of adenosylcobalamin (dot−dashed line) is also shown in the figure for comparison.

decrease from 506 cm^{-1} in methylcobalamin to 471 cm^{-1} in ethylcobalamin. The frequency of the C−Co stretch is substantially lower in adenosylcobalamin, where the resonance Raman spectrum is characterized by double peaks at 443 and 429 cm^{-1} attributed to the C−Co stretch. The frequency shift in the nominal C−Co stretching mode between methyl- and ethylcobalamin is qualitatively and quantitatively similar to the changes that are observed for a number of CH_3-X and C_2H_5-X compounds with similar C−X frequencies and force constants.[9−15] Thus, the frequency changes observed for the cobalamins are typical of the exchange of an ethyl group for a methyl group and do not reflect any specific (e.g. steric) destabilizing interaction between the ethyl group and the corrin ring. In addition, the modest change in C−Co force constant cannot, with any confidence, be extrapolated to indicate a significant change in bond dissociation energy.[16]

The additional decrease in the frequency of the C−Co stretch in adenosylcobalamin may reflect a steric destabilization of the C−Co bond as a result of interactions between the bulky adenosyl group and the corrin ring substituents.[5,6] However, the vibrational frequency is relatively insensitive to factors that control the ultimate bond dissociation energy. In particular, the observed vibrational frequency has little dependence on the presence or absence of the trans axial ligand, while the ultimate dissociation energy depends strongly on the presence or absence of the trans axial ligand.[17,18]

The photochemistry of alkylcobalamins provides another probe of the effect of the alkyl ligand on electronic structure and reactivity. It has long been known that photolysis of alkylcobalamins under anaerobic conditions results in the homolytic cleavage of the carbon−cobalt bond to form an alkyl radical and a cob(II)alamin radical. Photolysis occurs with substantial quantum yields, ranging from 0.1 to 0.5 for 6-coordinate base-on cobalamins.[19−22] Recently we reported data demonstrating distinctly different dynamics for the primary photolysis of methyl- and adenosylcobalamin. Excitation of methylcobalamin results in the wavelength dependent formation of two distinct primary photoproducts.[23,24] Following excitation at 400 nm ca. 25% of the initially excited methylcobalamin molecules undergo prompt bond homolysis forming methyl radical and cob(II)alamin. The remaining 75% of the initially excited methylcobalamin molecules form a metastable photoproduct with an absorption spectrum that is consistent with the formation of a cob(III)alamin species. The observation of a prominent blue shifted γ band centered at 340 nm suggests that this metastable photoproduct is a cob(III)alamin species with a very weak axial ligand. The picosecond transient absorption data may be interpreted in terms of heterolytic cleavage of the carbon−cobalt bond to form an ion pair between a five-coordinate cob(III)alamin and a methyl anion, or alternatively, in terms of population trapped in a localized (i.e. ion-pair-like) metal-to-ligand charge transfer state (MLCT state). In light of all of the observations, including those reported here, the latter alternative appears most likely. On a 1 ns time scale 12 ± 2% of the MLCT photoproduct forms cob(II)alamin, while the remainder returns to the ground state.

Following excitation of methylcobalamin near 520 nm in the visible $\alpha\beta$ band, only the MLCT photoproduct is observed at early times. On a 1 ns time scale the population partitions between the formation of cob(II)alamin (17% +3%/−5%) and ground-state recovery. These results suggest that the quantum yield for bond homolysis in methylcobalamin is determined by the wavelength-dependent partitioning between prompt homolysis and formation of the metastable photoproduct and by the partitioning of the metastable photoproduct between bond homolysis and ground-state recovery.

Similar transient absorption studies of adenosylcobalamin gave distinctively different results.[24−26] The principal photoproduct observed following excitation of adenosylcobalamin at 400 or 520 nm is cob(II)alamin. Unlike methylcobalamin, the photolysis quantum yield in adenosylcobalamin is determined

(8) Dong, S.; Padmakumar, R.; Banerjee, R.; Spiro, T. G. *J. Am. Chem. Soc.* **1999**, *121*, 7063−7070.
(9) Duncan, J. L.; Allan, A.; McKean, D. C. *Mol. Phys.* **1970**, *18*, 289−303.
(10) Crowder, G. A. *J. Mol. Spectrosc.* **1973**, *48*, 467−474.
(11) Hale, M. O.; Galicia, G. E.; Glogover, S. G.; Kinsey, J. L. *J. Phys. Chem.* **1986**, *90*, 4997−5000. Sundberg, R. L.; Imre, D.; Hale, M. O.; Kinsey, J. L.; Coalson, R. D. *J. Phys. Chem.* **1986**, *90*, 5001−5009.
(12) Phillips, D. L.; Myers, A. B. *J. Chem. Phys.* **1991**, *95*, 226−243. Phillips, D. L.; Lawrence, B. A.; Valentini, J. J. *J. Phys. Chem.* **1991**, *95*, 9085−9091. Phillips, D. L.; Myers, A. B.; Valentini, J. J. *J. Phys. Chem.* **1992**, *96*, 2039−2044.
(13) Shimanouchi, T. *Tables of Molecular Vibrational Frequencies*; Consolidated Volume I; National Bureau of Standards: Washington, DC, 1972.
(14) Synder, R. G.; Schachtschneider, J. H. *J. Mol. Spectrosc.* **1969**, *30*, 290−309.
(15) Dempster, A. B.; Zerbi, G. *J. Mol. Spectrosc.* **1971**, *39*, 1−7.
(16) Zhu, Q.; Cao, J. R.; Wen, Y.; Zhang, J.; Zhong, X.; Huang, Y.; Fang, W.; Wu, X. *Chem. Phys. Lett.* **1988**, *144*, 486-492. In this paper, gas-phase photodissociation studies of alkyl iodides accompanied by time-of-flight analysis of the translational energy of the photofragments provide bond dissociation energies of 55.0 ± 0.5 kcal/mol for methyl iodide and 55.3 ± 1.0 kcal/mol for ethyl iodide. Since the force constant changes and observed frequency shifts between methyl and ethyl iodide are almost identical with those reported for methyl and ethyl cobalamin it is obviously impossible to conclude that these force constant changes portend large changes in the bond dissociation energies.
(17) Hay, B. P.; Finke, R. G. *J. Am. Chem. Soc.* **1986**, *108*, 4820−4829.
(18) Hay, B. P.; Finke, R. G. *J. Am. Chem. Soc.* **1987**, *109*, 8012−8018.
(19) Hogenkamp, H. P. C. In B_{12}; Dolphin, D., Ed.; John Wiley and Sons: New York, 1982; Vol. 1, p295.
(20) Pratt, J. M.; Whitear, B. R. D. *J. Chem. Soc.* (*A*) **1971**, 252.
(21) Taylor, R. T.; Smucker, L.; Hanna, M. L.; Gill, J. *Arch. Biochem.* **1973**, 521.
(22) Chen, E.; Chance, M. R. *Biochemistry* **1993**, *32*, 1480−1487.
(23) Walker, L. A., II; Jarrett, J. T.; Anderson, N. A.; Pullen, S. H.; Matthews, R. G.; Sension, R. J. *J. Am. Chem. Soc.* **1998**, *120*, 3597.
(24) Shiang, J. J.; Walker, L. A., II; Anderson, N. A.; Cole A. G.; Sension, R. J. *J. Phys. Chem. B* **1999**, *103*, 10532−10539.
(25) Walker, L. A., II; Shiang, J. J.; Anderson, N. A.; Pullen, S. H.; Sension, R. J. *J. Am. Chem. Soc.* **1998**, *120*, 7286−7292.
(26) Yoder, L. M.; Cole, A. G.; Walker, L. A., II; Sension, R. J. *J. Phys. Chem. B.* In press.

by competition between geminate recombination and diffusion to form solvent-separated radical pairs.

An important question that arises from these findings is how the alkyl ligand affects photoproduct formation and state ordering in cobalamins. The effect of the alkyl ligand on state ordering and photolysis pathway may reflect features of alkylcobalamins relevant to the differing reactivities of methyl- and adenosylcobalamin dependent enzymes and to the control of reactivity by a protein. To investigate these questions further we have extended our time-resolved spectroscopic studies to include ethyl- and *n*-propylcobalamin. The present paper reports on the photolysis of ethyl- and *n*-propylcobalamin following excitation at 400 and 520 nm, and compares the photolysis mechanism in these cobalamins with the previously described results for methylcobalamin and adenosylcobalamin.

Experimental Methods

Sample Preparation. Synthesis and purification of ethyl- and *n*-propylcobalamin were carried out according to literature methods.[27,28] Cob(I)alamin was formed by the reaction of 170 mg of hydroxocobalamin with excess sodium borohydride in 12.5 mL of water and reacted with an excess of *n*-propyl bromide or ethyl iodide. The purity of the alkyl halide reactants was checked by NMR and found to be >99%. The product was desalted via extraction into 7.5 mL of a 50/50 w/v solution of phenol and methylene chloride. The organo-halide phase was then added, dropwise, to 40 mL of ethyl ether. The ether/cobalamin suspension was centrifuged, and the supernatant discarded. The product was redissolved in water and washed repeatedly with ethyl ether. Following evaporation of the residual ether, the aqueous solution could be used directly or dried in vacuo for storage. The UV−visible absorption spectra of these products matched those reported by Taylor et al. for ethyl- and *n*-propylcobalamin.[21] The resonance Raman spectrum of the propylcobalamin sample matched methylcobalamin in the 1000−1600 cm^{-1} region, indicating that the product is a base-on alkylcobalamin.[29] HPLC was performed according to the protocol of Jacobsen et al.,[30] using a C18 reverse phase column, 256 nm detection, and gradient elution. The gradient system consisted of 0.05 M phosphoric acid buffer at pH 3.0 (titrated using ammonium hydroxide) and acetonitrile. Following injection of the cobalamin onto the column, the gradient was developed via an increase of the acetonitrile concentration from 5% to 50% over 36 min at 1 mL/min flow rate. Hydroxo-, methyl-, ethyl-, and *n*-propylcobalamins all possess distinct elution times (10.1, 20.6, 22.5, and 23.2 min, respectively), and our ethyl- and *n*-propylcobalamin samples each yielded a single major peak having greater than 95% of the area. No evidence of the hydroxocobalamin starting material was observed in the HPLC.

Steady State and Time-Resolved Spectral Measurements. An accurate cob(II)alamin − propylcobalamin difference spectrum was determined as described previously.[23] The UV−visible absorption spectra of ethylcobalamin and *n*-propylcobalamin are nearly indistinguishable, thus the static difference spectra are also indistinguishable. The steady-state spectra of cob(II)alamin, methylcobalamin, *n*-propylcobalamin, and adenosylcobalamin are shown in Figure 1.

Transient absorption measurements were performed using a regeneratively amplified femtosecond Titanium sapphire laser as described in detail previously.[23,24,26,31] The excitation pulse was produced by generating the second harmonic of the laser at 400 nm, or by using a home-built optical parametric amplifier (OPA) to produce excitation pulses between 520 and 530 nm. The probe pulse was generated either by continuum generation in ethylene glycol or by using a second OPA. The probe pulses were delayed with respect to the pump pulses by a 1.5 m computer controlled motorized translation stage (Newport-Klinger). This stage allows measurements to be made with femtosecond resolution (1 μm step size = 6.67 fs of delay) out to a maximum time delay of ca. 10 ns. Traces were collected from −10 ps to 9 ns using variable time steps to resolve dynamics on time scales ranging from subpicoseconds to nanoseconds.[24,26] All measurements were performed with a magic angle polarization geometry.

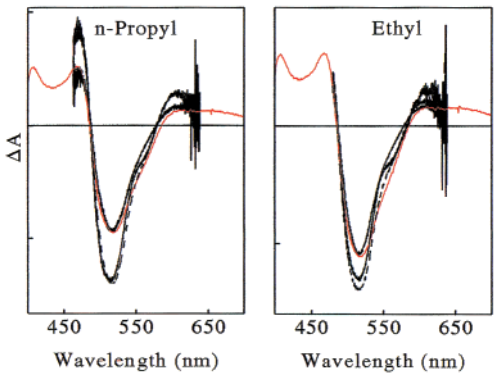

Figure 2. Comparison of transient difference spectra obtained following excitation of ethyl and *n*-propylcobalamin at 400 nm. Spectra are shown for time delays of 15, 100 (dashed line), and 800 ps. The 800 ps spectra are scaled for comparison with the steady state difference spectra (red lines).

For the transient absorption measurements ca. 2 mM solutions were prepared under anaerobic conditions achieved by bubbling argon through doubly distilled deionized water for at least 1 h prior to addition of the alkylcobalamin sample. Samples were dissolved in water or in pH 7 imidazole buffered aqueous solution. The dissolved samples were placed in a reservoir under an argon atmosphere and circulated with a flow rate sufficient to ensure that the sample volume was refreshed between laser shots. The reservoir was kept in an ice bath to prevent thermal degradation of the sample. UV−visible spectra taken before and after laser exposure were the same, ensuring that the sample integrity was maintained during each experiment.

Results

Transient Spectroscopic Measurements of Ethylcobalamin and *n*-Propylcobalamin. Pump−probe transient difference spectra of ethylcobalamin and *n*-propylcobalamin were collected at 10 ps (ethyl only), 15 ps, 25 ps, 50 ps, 100 ps, 200 ps, 400 ps, 800 ps, and 5 ns (*n*-propyl only) following excitation at 400 nm. The transient difference spectra obtained between 15 ps and 5 ns following excitation of *n*-propylcobalamin are included in Supporting Information. Transient difference spectra obtained 15, 100, and 800 ps following excitation of ethyl and *n*-propylcobalamin are shown in Figure 2 along with the steady-state difference spectrum expected for the formation of cob(II)alamin.

For all of the time delays measured, the transient difference spectra obtained following excitation of ethyl- and *n*-propylcobalamin are characteristic of the formation of cob(II)alamin and an alkyl radical. The difference spectrum projected to 5 ps by using kinetics measurements (vide infra) suggests that the bond homolysis is complete within a few picoseconds. A modest spectral evolution, characterized primarily by a <5 nm red shift of the peak of the bleaching signal, is evident in the transient absorption spectra obtained between 15 and 50 ps. A small evolution in the shape of the difference spectrum, slightly more

(27) Chemaly, S. M.; Pratt, J. M. *J. Chem. Soc., Dalton* **1980**, 2259.
(28) Kim, S.-H.; Chen. H. L.; Feilchenfeld, N.; Halpern, J. *J. Am. Chem. Soc.* **1988**, *110*, 3120.
(29) Salama, S.; Spiro, T. G. *J. Raman Spectrosc.* **1977**, *6*, 57.
(30) Jacobsen, D. W.; Green, R.; Quandros, E. V.; Montejano, Y. D. *Anal. Biochem.* **1982**, *120*, 394.
(31) Pullen, S.; Walker, L. A., II; Sension, R. J. *J. Chem. Phys.* **1995**, *103*, 7877.

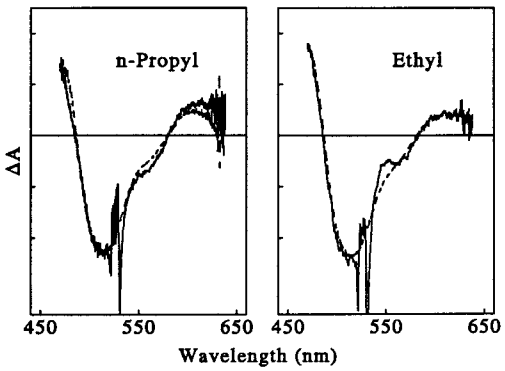

Figure 3. Transient difference spectra for ethyl- and *n*-propylcobalamin cobalamin obtained for a delay time of 40 ps (100 ps for *n*-propyl dashed line) following excitation at 530 ± 5 (solid lines) and 400 nm (dashed lines). The data in the region around 530 nm show some contamination from scatter of the 530 nm pump pulse.

prominent in ethylcobalamin than in *n*-propylcobalamin, is also observed in the spectral region around 550 nm. No significant evolution in the difference spectrum is evident between 100 ps and 5 ns. Over this time period the dynamics are characterized by a change in the absolute amplitude of the difference spectrum indicative of geminate recombination. The presence of a deviation between the steady state difference spectra and the transient difference spectra around 570 nm should also be noted. This difference will be discussed in more detail below.

Transient difference spectra obtained 40 ps following excitation of ethyl- and *n*-propylcobalamin at 530 nm are shown in Figure 3. These difference spectra are compared with data obtained following excitation at 400 nm. In both cases the observed difference spectrum is consistent with at least partial formation of cob(II)alamin and an alkyl radical within 40 ps. The *n*-propylcobalamin difference spectrum at 40 ps has only a slight dependence on excitation wavelength. The ethylcobalamin difference spectrum exhibits a prominent feature at ca. 550 nm, suggesting the presence of an intermediate in the bond homolysis pathway.

Narrow Bandwidth Transient Absorption Measurements of Ethylcobalamin and *n*-Propylcobalamin. In addition to the spectral measurements, kinetic data over a 9 ns window were obtained at 470, 520, 560, and 600 nm following excitation at 400 nm, and at 470, 520, 550, 560, and 600 nm following excitation at 520 nm. Typical data are illustrated in Figure 4. A more complete data set for *n*-propylcobalamin excited at 400 nm is included as Supporting Information.

For both ethyl- and *n*-propylcobalamin the traces obtained following excitation at 400 and 520 nm are qualitatively similar, with fast transients around zero time delay followed by a biexponential growth of the signal and a ca. 500 to 600 ps decay to a long-lived plateau. However, the growth in the magnitude of the bleach is significantly more pronounced and slower following excitation at 520 nm than 400 nm. This wavelength dependence is stronger in ethylcobalamin than in *n*-propylcobalamin. The contrast between ethyl- and *n*-propylcobalamin is illustrated more clearly in the kinetic traces probed at 560 nm (shown in Supporting Information). The traces obtained for *n*-propylcobalamin at this probe wavelength are almost indistinguishable following excitation at 400 and 520 nm, while the excitation wavelength dependence is pronounced in ethylcobalamin. These wavelength dependences are in good agreement

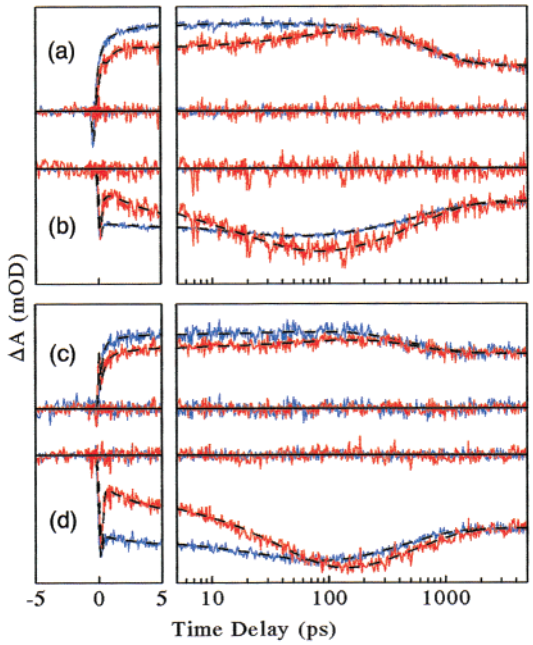

Figure 4. Comparison of transient kinetic measurements for *n*-propylcobalamin and ethylcobalamin with the multiexponential fit (dashed lines) as described in the text: (a) *n*-Propylcobalamin, 470 nm probe, (b) *n*-propylcobalamin, 520 nm probe, (c) ethylcobalamin, 470 nm probe, (d) ethylcobalamin, 520 nm probe. Red traces: 520 nm excitation. Blue traces: 400 nm excitation. The scans are offset for ease of comparison. The horizontal lines indicate zero absorbance change for each scan. Residuals between the fitted lines and the experimental data are also shown.

Table 1. Rate Constants, Time Constants (in parentheses), and Geminate Recombination Yields Obtained from the Fit of Transient Absorption Signals Following Excitation of Ethyl- and *n*-Propylcobalamin

	400 nm excitation		520 nm excitation	
	n-propyl	ethyl	*n*-propyl	ethyl
k_1 (ps^{-1})[a]	7.8 (130 fs)	8 (125 fs)	3.8 (260 fs)	5 (200 fs)
k_2 (ps^{-1})[a]	0.72 (1.4 ps)	0.71 (1.4 ps)	0.27 (3.7 ps)	0.38 (2.6 ps)
k_3 (ns^{-1})[a]	50 (20 ps)	55 (18 ps)	31 (32 ps)	21 (48 ps)
k_4 (ns^{-1})[a]	1.63 (614 ps)	1.94 (515 ps)	1.68 (594 ps)	2.00 (500 ps)
ϕ (at 9 ns)[b]	0.43 ± 0.08	0.62 ± 0.09	0.43 ± 0.08	0.61 ± 0.10

[a] The approximate error in the fitted parameters is ±10%. [b] The quantum yield is the mean value of ϕ (determined by eq 1) of all probe wavelengths. The reported uncertainty (precision only) is $\pm 1\sigma$.

with the differences observed in the 40 ps difference spectra illustrated in Figure 3.

The transient kinetic traces for each sample at each pump wavelength were fit to a sum of exponentials using a global analysis algorithm.[26] The global fitting of both ethyl- and *n*-propylcobalamin required the inclusion of an instrument limited Gaussian spike, 4 decay components, and a nondecaying component, although only a few traces required both the Gaussian spike and the fastest (<300 fs) decay component. Typical fits obtained for ethyl- and *n*-propylcobalamin are illustrated in Figure 4. The rate constants derived from these fits are given in Table 1. The amplitudes of the decay components are summarized as decay-associated difference spectra in the Supporting Information.

Following excitation at 400 nm the first three rate constants are essentially identical for *n*-propylcobalamin and ethylcobalamin. Collectively these rate constants describe internal conversion, bond cleavage, and thermalization of the initially excited

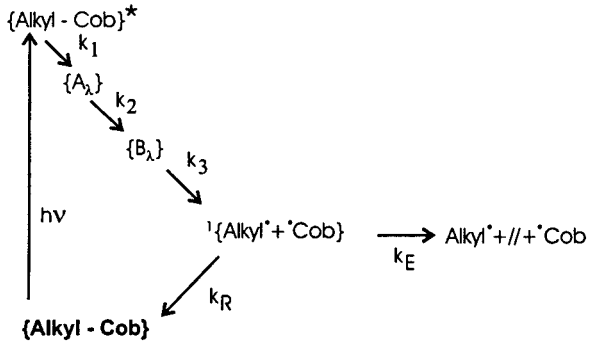

Figure 5. Schematic of the states involved in the photodissociation of ethyl- and *n*-propylcobalamin. Brackets represent molecular or solvent caged species. The longest rate constant is the sum of contributions due to geminate recombination and cage escape, $k_4 = k_R + k_E$.

cobalamin. The lack of dependence on the alkyl radical suggests that these rate constants reflect direct internal conversion and bond cleavage. In accord with the excitation wavelength dependence described above, the first three rate constants obtained following excitation at 520 nm exhibit a more pronounced dependence on the alkyl radical. The slowest rate constant (k_4) reflects geminate recombination of radical pairs and is independent of excitation wavelength, but dependent on the alkyl radical.

Photolysis Mechanism and the Geminate Recombination of Caged Radicals. A simple schematic mechanism for the photolysis of alkylcobalamins is illustrated in Figure 5. This mechanism is similar to the model used previously to account for the evolution of adenosylcobalamin in water and ethylene glycol.[26] Following excitation one or more excited states are populated. The excited states decay sequentially or in parallel to produce a solvent caged radical pair designated by {Alkyl· + ·Cob}. Competition between cage escape and geminate recombination accounts for the ultimate photolysis quantum yield for the production of solvent-separated radical pairs. Although one may imagine more complicated models to account for the observed data, the model outlined in Figure 5 contains the minimal number of distinctly observed intermediate states.

Given a model for the dynamics following excitation of ethyl- or *n*-propylcobalamin it is possible to use the measured rate constants and the observed decay associated spectra to construct the species associated difference spectra for each of the intermediate states as described previously.[26] The species associated difference spectra generated from the exponential fits are plotted in Figure 6. These spectra clearly illustrate the differences observed between 400 nm excitation and 520 nm excitation. Following excitation at 400 nm a difference spectrum characteristic of a cob(II)alamin species is formed on a time scale of approximately 125 fs. Modest evolution of the spectrum is observed on time scales of 1.4 and 20 ps. These data suggest prompt bond homolysis from a directly dissociative excited state following excitation at 400 nm. The subsequent 1.4 and 20 ps dynamics reflect relaxation of the hot corrin. Competition between geminate recombination and escape from the solvent cage occurs on a 500 to 600 ps time scale depending on the alkyl radical.

The initial dynamics observed following excitation in the $\alpha\beta$ band at 520 nm are significantly different. The earliest distinct intermediate, $\{A_{520}\}$, which is formed on a 200 to 300 fs time scale, has a cob(III)alamin-like spectrum reminiscent of the long-

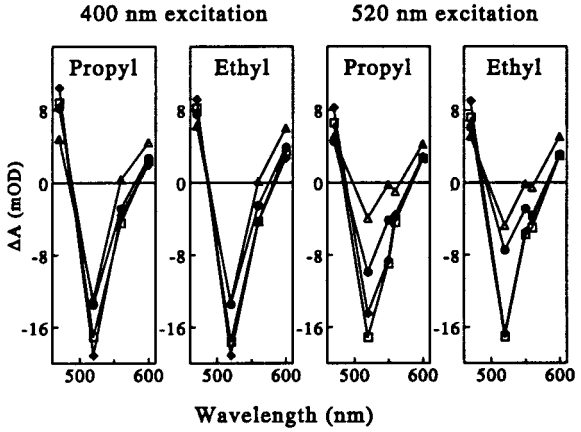

Figure 6. Species associated difference spectra for ethyl- and *n*-propylcobalamin following excitation at 400 and 520 nm derived from the model in Figure 5: △, $\{A_\lambda\}$; ●, $\{B_\lambda\}$; □, {Alkyl· + ·Cob}; ◆, Alkyl· +\\+ ·Cob.

lived intermediate observed following excitation of methylcobalamin.[24] The spectrum of the second distinct intermediate, $\{B_{520}\}$, is transitional between a cob(II)alamin-like and a cob(III)alamin-like difference spectrum. The picosecond evolution from $\{A_{520}\}$ to $\{B_{520}\}$ may reflect evolution from one electronic state to another, or it may reflect fast bond homolysis in competition with thermal relaxation of the initial cob(III)alamin-like intermediate state. In the latter interpretation, $\{B_{520}\}$ is a mixture of a cob(III)alamin species and caged radical pairs. The remaining cob(III)alamin intermediates undergo bond homolysis on a ca. 32 ps time scale in *n*-propylcobalamin and a ca. 48 ps time scale in ethylcobalamin.

The rate constant for the subnanosecond decay of the difference spectrum, describing the competition between geminate recombination and cage escape, is wavelength independent, but dependent on the alkyl radical: $k_4^{-1} = 604 \pm 55$ ps for *n*-propyl radical and 508 ± 35 ps for ethyl radical. As described previously,[26] the ratio of the amplitude of the plateau to the amplitude of the long decay, $R = S_P(\lambda)/S_4(\lambda)$, can be used along with the observed rate constants to determine the quantum yield, $\phi = k_E/k_4$, for cage escape by relaxed radical pairs according to eq 1:

$$\phi = \frac{QR}{1 + QR} \tag{1}$$

where $Q = k_1k_2k_3/[(k_1 - k_4)(k_2 - k_4)(k_3 - k_4)]$. The cage escape quantum yield at 9 ns for each wavelength is calculated according to eq 1, and the mean value is reported for each data set in Table 1. It should be noted that on the time scale of the experiments, components with time constants longer than 9 ns cannot be detected, so the possibility of diffusional recombination at very long times may affect the ultimate quantum yield. The multiexponential fit to the present data set implies quantum yields of 0.61 ± 0.09 and 0.43 ± 0.08 for cage escape by ethyl and *n*-propyl radicals, respectively. Assuming a unit quantum yield for the production of caged radical pairs, these values suggest quantum yields for photoinduced bond homolysis that are consistently larger than the literature values of 0.43 ± 0.05 (ethylcobalamin) and 0.31 ± 0.04 (*n*-propylcobalamin).[21] The difference between the steady state and picosecond photolysis yields may reflect partial excitation and recovery of an inactive form of ethyl- or *n*-propylcobalamin (i.e. quantum yield for

prompt bond homolysis <1) or the presence of an additional nanosecond recombination component, unresolved in our present measurements. However, the discrepancy may also reflect a systematic error in the steady state photolysis measurements. It should be noted that the quantum yield for photolysis of adenosylcobalamin reported in ref 21 is substantially lower than that obtained in more recent measurements (0.11 ± 0.01[21] as compared with 0.19 ± 0.04 in the work of Chen and Chance[22]).

Semiempirical Molecular Orbital Calculations of Alkylcobalamins. To investigate the effect of the alkyl ligand on the ground state geometry and to estimate the effect on the electronic molecular orbitals of alkylcobalamins, PM3(TM) molecular orbital calculations were performed for methyl and ethyl model compounds using the Spartan package of programs. The model compounds consist of an equatorial ring system identical to the corrin ring, but lacking the functional groups around the ring. The model ring system is identical to that used previously by Zhu and Kostic.[32] The nitrogenous axial ligand was modeled with imidazole or with dimethylbenzimidazole. Because cobalamin is zwitterionic, the model system has a +1 charge. The compensating negative charge in cobalamin is located on the phosphate group linking the dimethylbenzimidazole base to the corrin ring.

Upon substitution of ethyl for methyl, a small (4.5 pm) extension of the C−Co bond was calculated. However, the alkyl ligand was observed to have only a very small (<40 cm^{-1}) effect on the energies of the highest occupied molecular orbital (HOMO) and lowest unoccupied molecular orbital (LUMO), despite the fact that the HOMO includes significant electron density between the cobalt and the axial carbon atom. These results are in reasonable agreement with recent DFT calculations on similar model systems.[33] The LUMO for ethyl is essentially identical to that of methylcobalamin. The alkyl ligand has a small effect on the shape of the electron density in the carbon−cobalt bond in the HOMO, but does not appear to be involved in either of the two lowest unoccupied molecular orbitals (LUMO or LUMO+1) or in the next-highest occupied molecular orbital (HOMO-1). Plots of the HOMOs and LUMOs are included in Supporting Information. The major absorption bands observed in alkylcobalamins are generally assigned to combinations of the HOMO → LUMO, HOMO − 1 → LUMO and HOMO → LUMO + 1 electronic transitions.[34] Therefore, the similarities in these orbitals are in agreement with the observed similarities in the electronic absorption spectra. These calculations suggest that changes in the ground-state geometry or electronic configuration of the cobalamin cannot be invoked to account for the differences in the observed photochemistry.

Discussion

Comparison of the Primary Photochemistry in Alkylcobalamins. Photolysis of ethyl- and *n*-propylcobalamin at 400 nm results in homolytic bond cleavage on an ultrafast time scale, with the photoproduct present at 15 ps spectroscopically identified as a cob(II)alamin species. The species associated difference spectra derived from exponential fits to the data suggest that the initial intermediate produced on a 125 fs time scale is a cob(II)alamin species. Somewhat slower bond homolysis is observed following excitation of ethyl- or *n*-propylcobalamin at 520 or 530 nm near the peak of the visible $\alpha\beta$ absorption band, with production of a cob(III)alamin-like intermediate on a 200−300 fs time scale and conversion to cob(II)alamin completed on a 30−50 ps time scale dependent on the alkyl radical.

These observations provide an interesting mix of contrast and similarity to the dynamics observed for methylcobalamin.[23,24] Excitation of methylcobalamin at 400 nm produces a 3 to 1 branching between a cob(III)alamin-like excited state and prompt bond homolysis, while excitation of methylcobalamin at 520 nm produces only a long-lived cob(III)alamin-like photoproduct. This cob(III)alamin photoproduct branches between ground-state recovery ($86 \pm 5\%$) and bond homolysis ($14 \pm 5\%$) on a 1.0 ± 0.1 ns time scale.[24]

The data for all three of the alkylcobalamins suggest the presence of a bound cob(III)alamin metal-to-ligand charge transfer (MLCT) state in the pathway to bond homolysis following excitation in the low-lying $\alpha\beta$ absorption band. The principal distinction between methyl-, ethyl-, and *n*-propylcobalamin lies not in the stable cobalamin itself, but in the relative stability of this MLCT state. The longer ethyl and *n*-propyl groups act as electron donors and destabilize the partial carbon anion in the MLCT state. Raising the energy of this state decreases the barrier for homolytic dissociation thereby increasing the rate constant for homolysis and decreasing the lifetime of the intermediate. Excitation at 400 nm opens a pathway for direct photohomolysis of the carbon−cobalt bond. This direct dissociation pathway is significant for methylcobalamin, and dominant for ethyl- and *n*-propylcobalamins.

In contrast to the simple alkylcobalamins discussed above, the photolysis of adenosylcobalamin in aqueous solution is independent of wavelength for excitation at 400 and 520 nm.[24] The initial distinct intermediate ({A} in ref 26) has a cob(III)alamin-like spectrum. The second distinct intermediate ({B} in ref 26) may also have a cob(III)alamin-like spectrum. However, neither of these intermediates show the distinct sharp structure leading to the hump in the difference spectrum near 540 or 550 nm characteristic of formation of the MLCT state in methyl-, ethyl- and *n*-propylcobalamin. In addition, at least four picosecond decay components (1.4, 14, 110, and 500 ps), rather than three, and an additional intermediate (denoted by {I}) are required to account for the adenosylcobalamin data.[26] Both the decay associated difference spectrum attributed to the 110 ps decay component and the species associated difference spectrum assigned to {I} have no analogue in the dynamics of ethyl- or *n*-propylcobalamin.

Effect of the Alkyl Radical on Geminate Recombination. For adenosyl-, ethyl-, and *n*-propylcobalamin the slowest observed rate constant is clearly identified with geminate recombination of caged radical pairs. The observed rate constants for recombination and cage escape and the 9 ns quantum yields for formation of solvent separated radical pairs for ethyl-, *n*-propyl-, and adenosylcobalamin are summarized in Table 2.

Estimates of the recombination parameters for methylcobalamin were obtained by subtracting dynamics attributed to the long-lived MLCT intermediate produced following excitation at 520 nm from the signal obtained at 400 nm, assuming that

(32) Zhu, L.; Kostić, N. *Inorg. Chem.* **1987**, *26*, 4194−4197.
(33) Jensen, K. P.; Sauer, S. P. A.; Liljefors, T.; Norrby, P.-O. *Organometallics* **2001**, *20*, 550−556.
(34) Giannotti, C. In B_{12}; Dolphin, D., Ed.; John Wiley and Sons: New York, 1982; Vol. 1, pp 393−430.

Table 2. Comparison of Cage Escape and Geminate Recombination Parameters for Alkylcobalamins

compd	k_4 (ns^{-1})	ϕ (at 9 ns)	k_R[a] (ns^{-1})	k_E[a] (ns^{-1})	τ_D[b] (ns)
methylcobalamin	6.0 ± 2.6	0.8 ± 0.1	1.3 ± 0.5	4.7 ± 2.5	≤ 0.5
ethylcobalamin	1.97 ± 0.14	0.61 ± 0.09	0.76 ± 0.16	1.21 ± 0.16	0.93
n-propylcobalamin	1.65 ± 0.16	0.43 ± 0.08	0.94 ± 0.16	0.71 ± 0.16	1.7
adenosylcobalamin	2.0 ± 0.2	0.284 ± 0.020	1.43 ± 0.21	0.57 ± 0.06	2.3

[a] k_R and k_E are calculated using $k_E = \phi k_4$ and $k_4 = k_R + k_E$. [b] $\tau_D = (k_E - k_{ST})^{-1}$, where $k_{ST} = 0.13\ ns^{-1}$ is the best estimate for singlet triplet conversion of the radical pair from ref 26.

100% of the signal using 520 nm pump and 75% of the signal using 400 nm pump is due to the MLCT state. Prior to subtraction, the scans were scaled according to the reported quantum yields for radical pair formation.[24] Error bars for the methylcobalamin parameters in Table 2 were estimated by considering the upper and lower limits for the quantum yields and for the branching between MLCT formation and direct homolysis following excitation at 400 nm. Obviously these values for geminate recombination and cage escape are rough estimates for methylcobalamin, however, it is clear that the caging fraction for methylcobalamin falls in the range $0 \leq F_C \leq 0.3$. There is no indication of a more substantial geminate recombination component in the data. The rate constant derived for geminate recombination of methyl radical with cob(II)alamin is the same order of magnitude, ca. 1 ns^{-1}, observed for the other alkylcobalamins.

The results reported here provide no evidence for the hypothesis that the geometry or nature of the alkyl radical plays a significant role in the intrinsic rate of recombination for solvent caged radical pairs. The rate constants for geminate recombination in aqueous solution fall within a factor of 2, between 0.76 ns^{-1} (1.3 ns time constant) and 1.4 ns^{-1} (700 ps time constant). This is a reasonable range that may reflect relatively small specific differences in the dynamics of the different alkyl radicals. However, the precision of the data precludes any reasonable attempt to interpret the observed differences in terms of radical properties.

Likewise, there is a clear qualitative trend in the data relating the size or volume of the alkyl radical with the observed rate constant for cage escape. Intrinsic cage escape occurs on time scales ranging from ≤ 0.5 ns for methyl radical to 2.3 ns for adenosyl, the largest radical studied. The rapid cage escape observed for the smallest radicals studied may be related to the enhanced ability of these radicals to diffuse in the relatively open, hydrogen-bonded local network of water.

Comparison of the Steady State and Nanosecond Transient Difference Spectra. As noted in the results section above, there is a systematic deviation between the steady state difference spectra for the formation cob(II)alamin from ethyl- or *n*-propylcobalamin and the transient difference spectra presented in Figure 2. The spectral signature of this difference is illustrated in Figure 7. It is tempting to attribute this deviation between the steady state and transient difference spectra to a very slow relaxation of the corrin ring in cob(II)alamin following photodissociation. However, no such change in the difference spectrum is observed following excitation of adenosylcobalamin as shown in the inset in Figure 7. It is therefore doubtful that the deviation arises from the cob(II)alamin species. The ethyl- and *n*-propylcobalamin difference spectra decay uniformly between 100 ps and 5 ns, with no evidence of significant evolution. This leads to the conclusion that the transient difference spectrum reflects the true difference spectrum for the photoactive alkylcobalamin undergoing geminate recombination, and that the deviation between the steady state and transient difference spectra in ethyl- and *n*-propylcobalamin may arise from the alkyl radical itself, possibly as a solvent−radical complex.

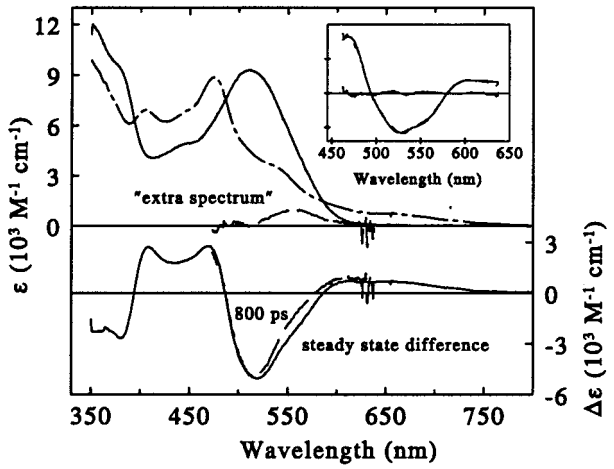

Figure 7. Comparison of the steady state (solid line) and transient (dashed line) difference spectra for *n*-propylcobalamin. Subtraction of the two yields the "extra spectrum" shown in comparison with the steady-state spectra of *n*-propylcobalamin (solid line) and cob(II)alamin (dot−dashed line). The inset compares the 900 ps transient (dashed line) and steady state (solid line) difference spectra for adenosylcobalamin. The subtraction of these two spectra leaves the residual around zero also shown in the figure.

Comparison of the steady state and transient difference spectra in ethyl- and *n*-propylcobalamin allows the presence of an additional absorption component peaking between 550 and 560 nm in these samples as illustrated in Figure 7. Because the steady state photolysis is performed in the presence of a radical scavenger (TEMPO), the alkyl radicals are not present and the steady state difference spectrum reflects only the absorption contribution due to the formation of cob(II)alamin. Therefore, any absorption arising from the radicals or from their complexes with water will be reflected as a discrepancy between the steady state and transient difference spectra. For the isolated radicals in the gas phase there is no evidence for a low-energy electronic absorption band in these alkyl species.[35] Likewise, millisecond transient spectra of isopropyl radicals in solution (hexadecane) show no absorption in the visible region.[36] However, steady-state spectra of ethyl and *n*-propyl radicals in water are unavailable and the effect of the solvent on their spectroscopy is unknown. Future ultrafast experiments designed to explore the dynamics and spectroscopy of transient alkyl radicals in solution may shed some light on the present contribution to the transient absorption spectrum of alkylcobalamins.

(35) Jacox, M. E. *Vibrational and electronic energy levels of polyatomic transient molecules*; American Chemical Society: Washington, DC; American Institute of Physics: New York; for the National Institute of Standards and Technology, 1994.
(36) Huggenberger, C.; Fischer, H. *Helv. Chim. Acta* **1981**, *64*, 338.

Conclusion

This paper presents a transient absorption study of the primary photolysis of ethyl- and *n*-propylcobalamin in water and a comparison of the photolysis of methyl-, ethyl-, *n*-propyl-, and adenosylcobalamin at two different excitation wavelengths. Excitation of methyl-, ethyl-, and *n*-propylcobalamin at 520 nm in the low-lying $\alpha\beta$ absorption band results in bond homolysis proceeding via a bound cob(III)alamin MLCT state. The principal distinction between methyl-, ethyl-, and *n*-propylcobalamin lies in the relative stability of this MLCT state, with the terminal alkyl groups in ethyl and *n*-propyl acting as electron donors to destabilize the partial carbon anion in the MLCT state. The lifetime of the MLCT state is inversely related to the size of the alkyl ligand: 1 ns (methyl), 48 ps (ethyl), 32 ps (*n*-propyl), and $\leq$14 ps (adenosyl, if the MLCT state is present). Excitation at 400 nm opens a pathway for direct photohomolysis of the carbon−cobalt bond in methyl-, ethyl-, and *n*-propylcobalamin. This direct dissociation pathway is significant for methylcobalamin, and dominant for ethyl- and *n*-propylcobalamins. In contrast the photolysis of adenosylcobalamin in aqueous solution is independent of wavelength for excitation at 400 and 520 nm.[24] The photolysis of adenosylcobalamin is also distinguished by the presence of an additional intermediate with a 110 ps lifetime that has no analogue in the other cobalamins studied.

Finally it should be noted that the cage recombination efficiency is a property of the specific alkyl radical with distinct differences observed for the geminate recombination of methyl-, ethyl-, *n*-propyl-, and adenosylcobalamin in aqueous solution. The results reported here provide no evidence for the hypothesis that the geometry or nature of the alkyl radical plays a significant role in the intrinsic rate of recombination for solvent caged radical pairs. The rate constants for geminate recombination in aqueous solution fall within a factor of 2, between 0.76 (1.3 ns time constant) and 1.4 ns^{-1} (700 ps time constant). Intrinsic cage escape occurs on time scales ranging from $\leq$0.5 ns for methyl radical to 2.3 ns for adenosyl, the largest radical studied.

The caging fraction for geminate recombination of radical pairs may be determined precisely for most of the compounds studied here. The solvent caging correlates well with the size of the radical following anticipated trends: $0 \leq F_C \leq 0.3$ for methyl radical, 0.4 for ethyl radical, 0.57 for *n*-propyl radical, and 0.72 for adenosyl radical.

Acknowledgment. This work is supported by NIH grant NIDDK 53842. J.J.S. was supported in part by the Fellows program of the Center for Ultrafast Optical Science NSF STC PHY 8920108. We would also like to thank Professor Rowena Matthews for enlightening discussions and access to equipment required to purify and characterize ethyl- and *n*-propylcobalamin.

Supporting Information Available: Figure S1, transient difference spectra for *n*-propylcobalamin from 15 ps to 5 ns; Figure S2, transient kinetic measurements of *n*-propylcobalamin; Figure S3, the decay associated difference spectra; Figure S4, a comparison of transient kinetics of ethyl- and *n*-propylcobalamin; and Figure S5, HOMOs and LUMOs for ethyl- and methylcobalamin (PDF). This material is available free of charge via the Internet at http://pubs.acs.org.

JA011628S